

Kink structure in the electronic dispersion of high- T_c superconductors from the electron-phonon interaction

Shigeru Koikegami*

Second Lab, LLC, 10-7-204 Inarimae, Tsukuba 305-0061, Japan

Nanoelectronics Research Institute, AIST Tsukuba Central 2, Tsukuba 305-8568, Japan

Yoshihiro Aiura

Nanoelectronics Research Institute, AIST Tsukuba Central 2, Tsukuba 305-8568, Japan

(Dated: today)

Abstract

We investigate the electronic dispersion of high- T_c superconductor on the basis of the two-dimensional three-band Hubbard model with the electron-phonon interaction together with the strong electron-electron interaction. In our model, it is shown across the hole-doped region of high- T_c superconductor that the electron-phonon interaction makes a dispersion kink, observed along the nodal direction, and that the small isotope effect appears on the electronic dispersion.

PACS numbers: 71.10.Fd, 71.38.-k, 74.20.Mn

INTRODUCTION

For the past two decades, extensive studies of high- T_c cuprates have spotlighted many curious phenomena. It has been argued that most phenomena are attributable to the strong correlations among electrons, which play significant roles in these materials. However, since the discovery of sudden changes in the electron dispersion or “kinks” shown by the angle-resolved photoemission spectroscopy (ARPES),^{1,2} effects of electron-boson interactions on electronic self-energies have been recognized. While the kinks are now indisputable in cuprates,³ their origin as arising from electronic coupling to phonons⁴ or magnetic excitations^{5,6,7} remains unclear.

Recent scanning tunneling microscope study showed that the statistical distribution of energy of bosonic modes (Ω) has meaningful difference between ^{16}O and ^{18}O materials. Thus, it should be hard to exclude the possibility that electron-phonon interaction (EPI) significantly affects the electronic states in cuprates.

In this study, we investigate the analysis upon the EPI together with the electron-electron interaction (EEI) on the basis of the two-dimensional (2D) three-band Hubbard–Holstein (HH) model. With the use of our three-band HH model, we can reproduce the situation of the real high- T_c materials, in which EPI mainly works on p electrons at O sites.

FORMULATION

Our model Hamiltonian H is composed of d electrons at each Cu site, p electrons at O site, and lattice vibrations of O atoms. We consider only the on-site Coulomb repulsion U between d electrons at each Cu site as our EEI. Let us define that μ and N_0 represent the chemical potential and the number of all electrons, respectively. Then, $H - \mu N_0$ is divided into the non-interacting part, H_0 , the electron-electron interacting part H_{el-el} , the phonon part H_{ph} , and the electron-phonon interacting part H_{el-ph} as

$$\begin{aligned}
 H - \mu N_0 &= H_0 + H_{el-el} + H_{ph} + H_{el-ph}, \\
 N_0 &= \sum_{\mathbf{k}\sigma} (d_{\mathbf{k}\sigma}^\dagger d_{\mathbf{k}\sigma} + p_{\mathbf{k}\sigma}^{x\dagger} p_{\mathbf{k}\sigma}^x + p_{\mathbf{k}\sigma}^{y\dagger} p_{\mathbf{k}\sigma}^y).
 \end{aligned}
 \tag{1}$$

Here, $d_{\mathbf{k}\sigma}$ ($d_{\mathbf{k}\sigma}^\dagger$) and $p_{\mathbf{k}\sigma}^{x(y)}$ ($p_{\mathbf{k}\sigma}^{x(y)\dagger}$) are the annihilation (creation) operator for d and $p^{x(y)}$ electrons of momentum \mathbf{k} and spin σ , respectively. The non-interacting part H_0 is represented

by

$$\begin{aligned}
H_0 &= \sum_{\mathbf{k}\sigma} \left(d_{\mathbf{k}\sigma}^\dagger p_{\mathbf{k}\sigma}^{x\dagger} p_{\mathbf{k}\sigma}^{y\dagger} \right) \begin{pmatrix} \Delta_{dp} & \zeta_{\mathbf{k}}^x & \zeta_{\mathbf{k}}^y \\ -\zeta_{\mathbf{k}}^x & 0 & \zeta_{\mathbf{k}}^p \\ -\zeta_{\mathbf{k}}^y & \zeta_{\mathbf{k}}^p & 0 \end{pmatrix} \begin{pmatrix} d_{\mathbf{k}\sigma} \\ p_{\mathbf{k}\sigma}^x \\ p_{\mathbf{k}\sigma}^y \end{pmatrix} \\
&\equiv \sum_{\mathbf{k}\sigma} \mathbf{d}_{\mathbf{k}\sigma}^\dagger \mathbf{H}_0 \mathbf{d}_{\mathbf{k}\sigma}.
\end{aligned} \tag{2}$$

We take the lattice constant of the square lattice formed from Cu sites as the unit of length. Then, $\zeta_{\mathbf{k}}^{x(y)} = 2i t_{dp} \sin \frac{k_{x(y)}}{2}$ and $\zeta_{\mathbf{k}}^p = -4t_{pp} \sin \frac{k_x}{2} \sin \frac{k_y}{2}$, where t_{dp} is the transfer energy between a d orbital and a neighboring $p^{x(y)}$ orbital and t_{pp} is that between a p^x orbital and a p^y orbital. Δ_{dp} is the difference of energy levels of d and p orbitals. In this study, we take t_{dp} as the unit of energy. The residual parts are described as follows:

$$H_{el-el} = \frac{U}{N} \sum_{\mathbf{k}\mathbf{k}'} \sum_{\mathbf{q}(\neq 0)} d_{\mathbf{k}+\mathbf{q}\uparrow}^\dagger d_{\mathbf{k}'-\mathbf{q}\downarrow}^\dagger d_{\mathbf{k}'\downarrow} d_{\mathbf{k}\uparrow}, \tag{3}$$

$$H_{ph} = \sum_{\mathbf{q}} \sum_{\nu=\{x,y\}} \omega_{\mathbf{q}}^\nu b_{\mathbf{q}}^{\nu\dagger} b_{\mathbf{q}}^\nu, \tag{4}$$

and

$$H_{el-ph} = \frac{1}{N} \sum_{\mathbf{k}\sigma} \sum_{\mathbf{q}} \sum_{\nu=\{x,y\}} g \alpha_{\mathbf{k},\mathbf{q}}^\nu p_{\mathbf{k}+\mathbf{q}\sigma}^{\nu\dagger} p_{\mathbf{k}\sigma}^\nu (b_{\mathbf{q}}^\nu + b_{-\mathbf{q}}^{\nu\dagger}), \tag{5}$$

where U is the on-site Coulomb repulsion between d orbitals, N is the number of \mathbf{k} -space lattice points in the first Brillouin zone (FBZ), and $g \alpha_{\mathbf{k},\mathbf{q}}^\nu$ ($\nu = \{x, y\}$) is the electron-phonon matrix element, respectively. We consider that the half-breathing phonon mode,⁹ in which oxygen ions are vibrating along the x or y directions, is crucial for our problem. Thus, ignoring the other phonon modes, we have the electron-phonon interacting part as Eq. (5).

Then, we introduced the unperturbed and perturbed Green's functions, which are to be described in 3×3 matrix form. The unperturbed Green's function $\mathbf{G}^{(0)}(\mathbf{k}, z)$ is derived from Eq. (2) as

$$\mathbf{G}^{(0)}(\mathbf{k}, z) = [z\mathbf{I} - \mathbf{H}_0]^{-1}, \tag{6}$$

where \mathbf{I} is a 3×3 unit matrix. Using the abbreviation of Fermion Matsubara frequencies, $\epsilon_n = \pi T(2n + 1)$ with integer n and temperature T , the perturbed Green function $\mathbf{G}(\mathbf{k}, z)$ is determined by the Dyson equation:

$$\mathbf{G}(\mathbf{k}, i\epsilon_n)^{-1} = \mathbf{G}^{(0)}(\mathbf{k}, i\epsilon_n)^{-1} - \Sigma(\mathbf{k}, i\epsilon_n), \tag{7}$$

where $\Sigma(\mathbf{k}, i\epsilon_n)$ is the self-energy expected to be a diagonal matrix. In order to estimate the d electron self-energy $\Sigma_d(\mathbf{k}, i\epsilon_n) \equiv \Sigma_{11}(\mathbf{k}, i\epsilon_n)$ in Eq. (7), we adopt the fluctuation exchange approximation¹⁰ as follows:

$$\Sigma_d(\mathbf{k}, i\epsilon_n) = \frac{T}{N} \sum_{\mathbf{q}m} G_d(\mathbf{k} - \mathbf{q}, i\epsilon_n - i\omega_m) V_{\text{el-el}}(\mathbf{q}, i\omega_m), \quad (8)$$

where $G_d(\mathbf{k}, i\epsilon_n) \equiv G_{11}(\mathbf{k}, i\epsilon_n)$,

$$V_{\text{el-el}}(\mathbf{q}, i\omega_m) = \frac{3}{2} \frac{U^2 \chi(\mathbf{q}, i\omega_m)}{1 - U \chi(\mathbf{q}, i\omega_m)} + \frac{1}{2} \frac{U^2 \chi(\mathbf{q}, i\omega_m)}{1 + U \chi(\mathbf{q}, i\omega_m)} - U^2 \chi(\mathbf{q}, i\omega_m), \quad (9)$$

where $\omega_m = 2m\pi T$ with integer m are Boson Matsubara frequencies, and

$$\chi(\mathbf{q}, i\omega_m) = -\frac{T}{N} \sum_{\mathbf{k}n} G_d(\mathbf{q} + \mathbf{k}, i\omega_m + i\epsilon_n) G_d(\mathbf{k}, i\epsilon_n). \quad (10)$$

In order to estimate the $p^{x(y)}$ -electron self-energy $\Sigma_{x(y)}(\mathbf{k}, i\epsilon_n) \equiv \Sigma_{22(33)}(\mathbf{k}, i\epsilon_n)$ in Eq. (7), we exploit the Brillouin-Wigner perturbation theory. We adopt the self-consistent one-loop approximation as follows:

$$\Sigma_{x(y)}(\mathbf{k}, i\epsilon_n) = \frac{T}{N} \sum_{\mathbf{q}m} G_{x(y)}(\mathbf{k} - \mathbf{q}, i\epsilon_n - i\omega_m) V_{\text{el-ph}}^{x(y)}(\mathbf{q}, i\omega_m), \quad (11)$$

where $G_{x(y)}(\mathbf{k}, i\epsilon_n) \equiv G_{22(33)}(\mathbf{k}, i\epsilon_n)$ and $V_{\text{el-ph}}^{x(y)}(\mathbf{q}, i\omega_m)$ is the EPI on $p^{x(y)}$ electron. Our EPI is determined as follows:

$$V_{\text{el-ph}}^{x(y)}(\mathbf{q}, i\omega_m) = \lambda \left| \alpha_{\mathbf{q}}^{x(y)} \right|^2 \left[\frac{1}{\omega_h + i\omega_m} + \frac{1}{\omega_h - i\omega_m} \right], \quad (12)$$

where $\lambda = g^2/(2\omega_h)$ and $\alpha_{\mathbf{q}}^{x(y)} = \sin \frac{q_{x(y)}}{2}$. ω_h is the specific phonon energy for the half-breathing mode. As above, we ignore the effects in which EEI and EPI are coupled. Thus, as shown by Eqs. (8)-(12), in our formulation, EEI and EPI are completely decoupled. Of course, this assumption is inadequate to analyze the case in which the characteristic energy due to EEI is comparable to the phonon energy. However, as will be seen later, we actually treat the cases with rather high characteristic energy due to EEI. Hence, decoupling EEI with EPI should be justified in our analysis. The electron-phonon coupling constant λ does not depend on M_O since $\omega_h \propto M_O^{-1/2}$ and $g \propto (M_O \omega_h)^{-1/2}$, where M_O is the mass of an oxygen ion. In our model, thus, the isotope effect is reflected on the phonon energy in the electronic self-energies only, but not any changes in the strength.

Isotope	n_d^h	n_p^h	δ	
^{16}O	0.5575	0.4837	0.0412	LD
^{18}O	0.5574	0.4838	0.0412	LD
^{16}O	0.5932	0.5039	0.0971	UD
^{18}O	0.5931	0.5040	0.0972	UD
^{16}O	0.6281	0.5258	0.1540	OP
^{18}O	0.6281	0.5259	0.1540	OP
^{16}O	0.6683	0.5525	0.2209	OD
^{18}O	0.6683	0.5526	0.2209	OD

TABLE I: Number of doped holes. $\delta \equiv n_d^h + n_p^h - 1$.

RESULTS AND DISCUSSION

We need to solve Eqs. (7)–(11) in a fully self-consistent manner. During numerical calculations, we divide the FBZ into 128×128 meshes. We prepare $2^{12} = 4096$ Matsubara frequencies for temperature $T \sim 87\text{K}$. As shown later, at this temperature, our calculation can reproduce the important behavior of electrons in normal state. Moreover, to our knowledge, the situation will not be changed if we change T to some extent.

$t_{dp} \sim 1.0\text{ eV}$ and $t_{pp} \sim 0.55\text{ eV}$, which are all common for our calculations. These values are chosen so that we can reproduce the typical Fermi surface of $\text{Bi}_2\text{Sr}_2\text{CaCu}_2\text{O}_{8+\delta}$ observed by ARPES.^{11,12} $\Delta_{dp} \sim 1.4\text{ eV}$, $U \sim 3.0\text{ eV}$, and $\lambda = 0.8$ unless stated. The phonon energy is set as $\omega_h \sim 65(61)\text{ meV}$ for $^{16}\text{O}(^{18}\text{O})$ material.

We show the numbers of doped holes for our fully self-consistent solutions in Table I. The numbers of doped holes both for ^{16}O and ^{18}O materials are exactly the same to three places of decimals and they correspond to four different hole-doped samples, lightly doped (LD), underdoped (UD), optimally doped (OP), and overdoped (OD), respectively. In Fig. 1, we show the color map of the one-particle spectrum at Fermi level $A(\mathbf{k}, 0)$, where

$$A(\mathbf{k}, \varepsilon) \equiv -\frac{1}{\pi} \text{Im} \{ \text{Tr} \mathbf{G}(\mathbf{k}, i\epsilon_n) \}_{i\epsilon_n \rightarrow \varepsilon}, \quad (13)$$

in order to indicate the Fermi surfaces for ^{16}O materials. In Eq. (13), the Padé approximation is exploited for analytic continuation. Furthermore, we calculate the electronic dispersions of

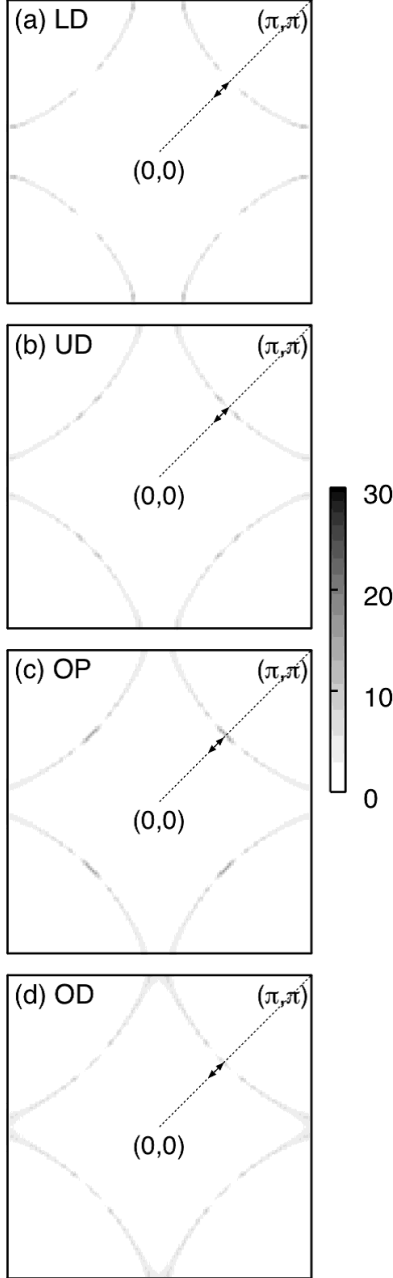


FIG. 1: Fermi surfaces for ^{16}O materials indicated in Table I.

the antibonding band $E_d(\mathbf{k})$ along the nodal direction indicated as the cut in Fig. 1 for all our doping cases. $E_d(\mathbf{k})$ is determined as the \mathbf{k} point on which $A(\mathbf{k}, \varepsilon)$ has the maximum value at each energy level. Due to this method, the curves of $E_d(\mathbf{k})$ look like a series of line segments, as shown in Fig. 2. We compare every $E_d(\mathbf{k})$ of our solution with the one obtained by another fully self-consistent manner, in which the same calculation is performed, except for the EPI. We show our results on these dispersions in Fig. 2, where we can easily recognize that the

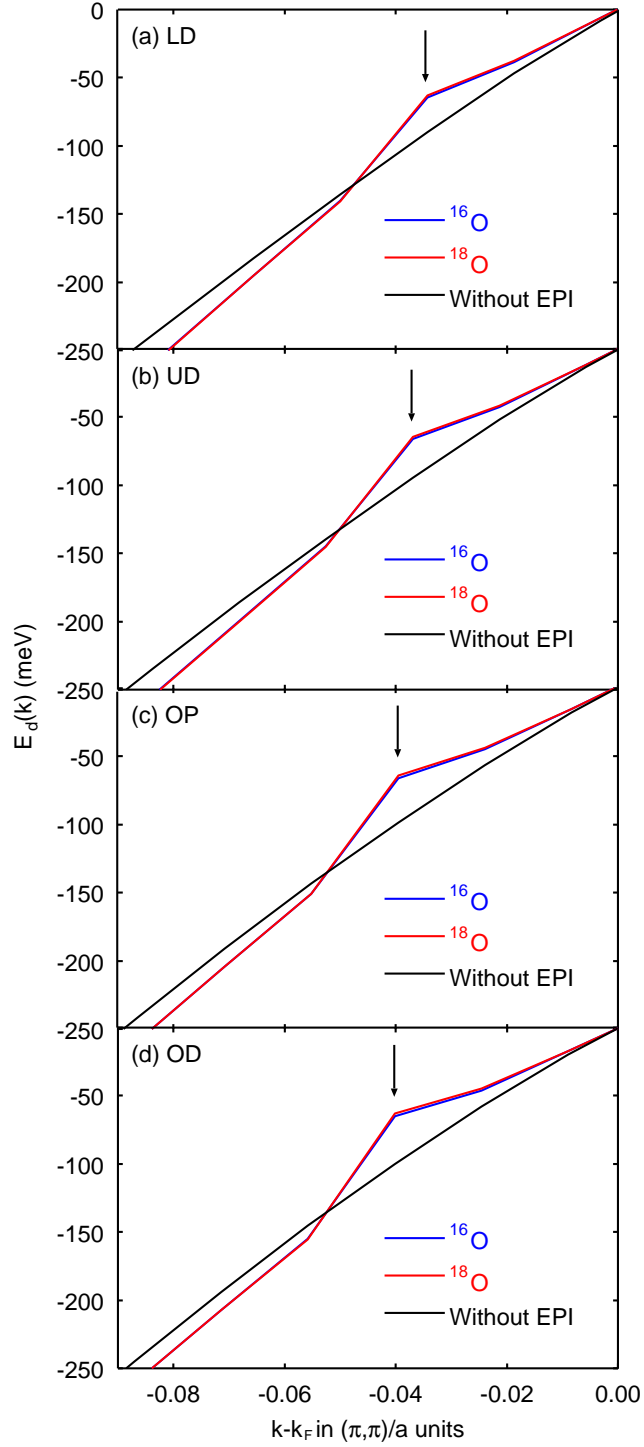


FIG. 2: Dispersion kinks along the nodal direction. Momentum is measured from each Fermi surface. Arrows indicate the momenta at which kinks occur.

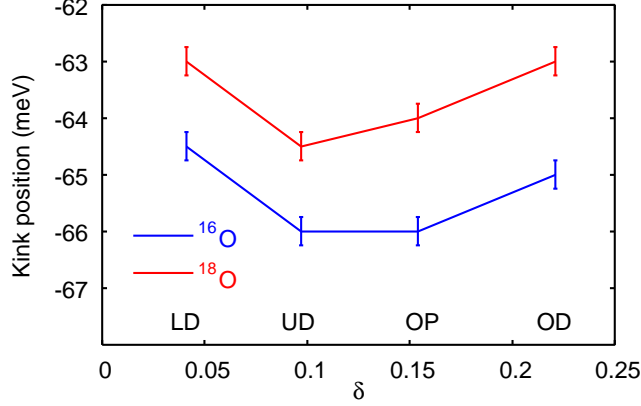


FIG. 3: Doping dependence of kink energies. Bars indicate the discretization error during analytic continuation.

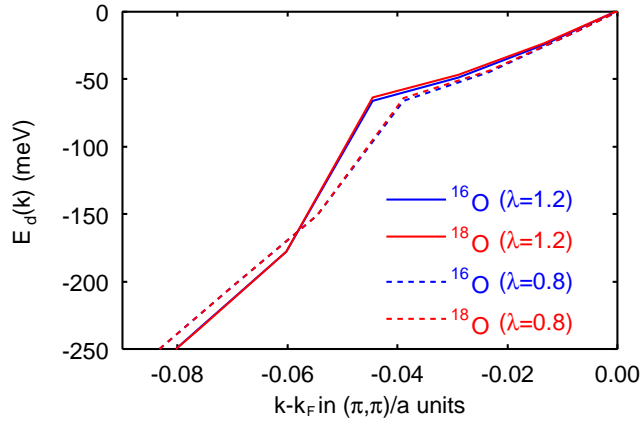


FIG. 4: Dispersion kinks along the nodal direction for $\lambda = 1.2$. The number of doped holes for ^{16}O (^{18}O) material is $\delta = 0.1309$ (0.1310). The dashed lines show the ones for OP in Table I.

dispersion kinks along the nodal direction appear only when EPI affects the $p^{x(y)}$ electrons. The kink energies were slightly shifted by $^{16}\text{O} \rightarrow ^{18}\text{O}$ substitution. In Fig. 3, we detail how these kink energies shift depending on hole doping. These theoretically evaluated isotope shifts are at most 2.5 meV, which are much smaller than the ones measured by another group's ARPES experiment.^{13,14} Furthermore, these isotope shifts are almost independent of hole doping while another group insists that they are critically affected.¹⁵ Considering the energy and momentum resolutions in their experiment, it may be hard to detect the subtle isotope shifts and their dependence on hole doping shown in our model.

Let us now look at λ and Δ_{dp} dependences in the dispersion kinks along the nodal direction in detail. Figure 4 shows the energy dispersions for $\lambda = 0.8$ (dotted lines) and $\lambda = 1.2$ (solid

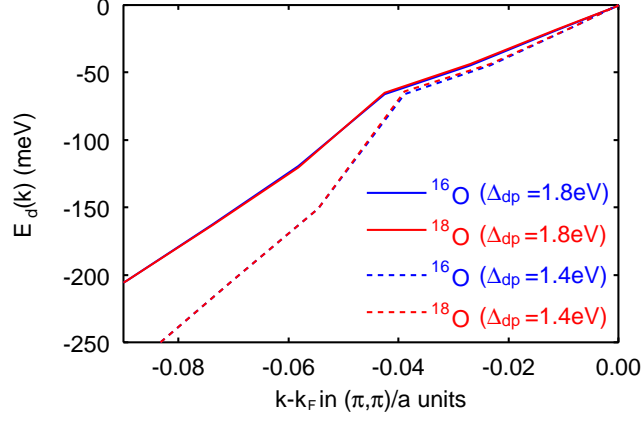


FIG. 5: Dispersion kinks along the nodal direction for $\Delta_{dp} = 1.8$ eV. The number of doped holes for ^{16}O (^{18}O) material is $\delta = 0.1621$ (0.1622). The dashed lines show the ones for OP in Table I.

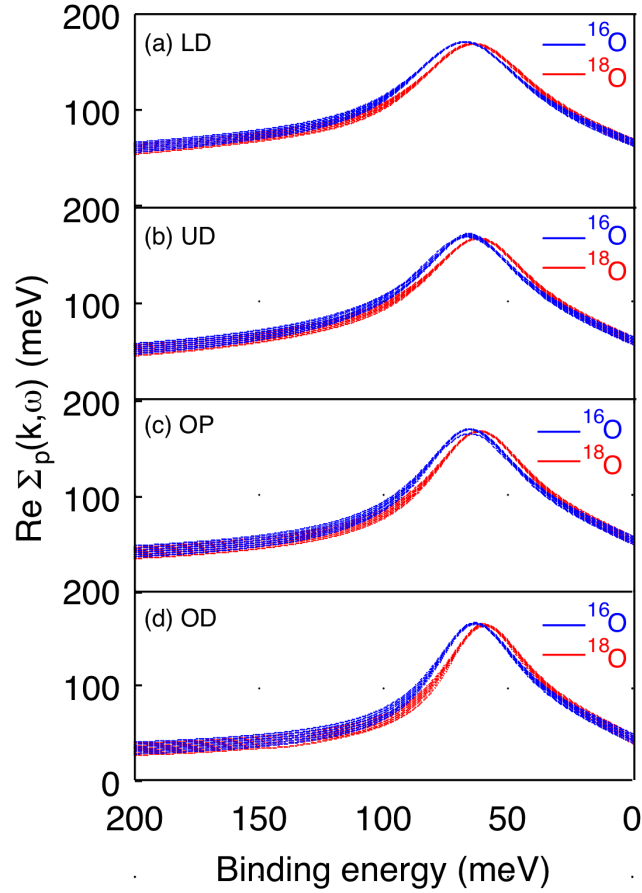


FIG. 6: $\Sigma_p(\mathbf{k}, \omega)$ on $\mathbf{k} = \left(\tilde{k}_F - \frac{n}{64}\right)(\pi, \pi)$ ($n = 0, 1, \dots, 5$), where $\tilde{k}_F = \frac{59}{128}$ for (a), $\tilde{k}_F = \frac{57}{128}$ for (b), $\tilde{k}_F = \frac{55}{128}$ for (c), and $\tilde{k}_F = \frac{53}{128}$ for (d), respectively.

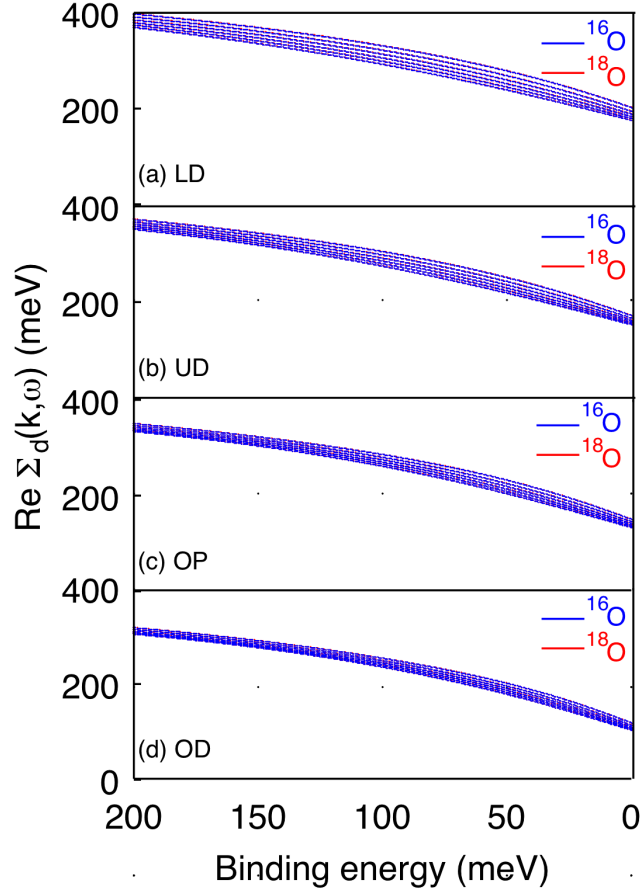


FIG. 7: $\Sigma_d(\mathbf{k}, \omega)$ on the same \mathbf{k} points as in Fig. 4.

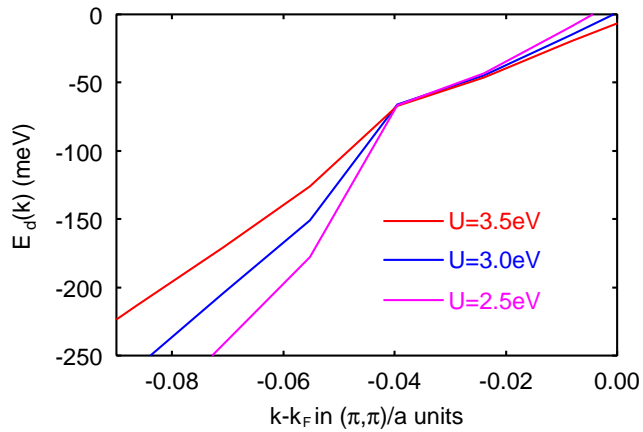


FIG. 8: Dispersion kinks along the nodal direction for $U = 2.5, 3.0,$ and 3.5 eV. They all correspond to OP. Momentum is measured from the Fermi surface for $U = 3.0$ eV.

lines). There is no clear difference in the isotope effect between $\lambda = 1.2$ (2.5 meV) and $\lambda = 0.8$ (2.0 meV), though the dispersion kinks for $\lambda = 1.2$ are distinctly shifted to the high binding energy compared with those for $\lambda = 0.8$. On the other hand, the isotope shift for $\Delta_{dp} = 1.8$ eV (1 meV) is slightly shrank compared to that for $\Delta_{dp} = 1.4$ eV (2.5 meV), though the dispersions depend on the Δ_{dp} considerably, as shown in Fig. 5. Hence, our model calculation shows that the isotope shifts are not sensitive to λ and Δ_{dp} . Considering that Δ_{dp} is closely related with EEI in our three band HH model as discussed later, we can be fairly certain that the isotope shifts are determined by the relative strength between EPI and EEI. However, these changes of the isotope shifts are minute, thus, our discussions so far are valid regardless of λ and Δ_{dp} .

To clarify the EPI effect on the $p^{x(y)}$ electrons described above, we investigate the p electron self-energy $\Sigma_p(\mathbf{k}, \omega) \equiv \Sigma_x(\mathbf{k}, \omega) + \Sigma_y(\mathbf{k}, \omega)$ along the nodal direction. In Fig. 6, we show $\Sigma_p(\mathbf{k}, \omega)$ on every six \mathbf{k} points along the nodal direction, located inside Fermi surfaces. The energy where $\Sigma_p(\mathbf{k}, \omega)$ is maximal corresponds to the one of the dispersion kink and shifts upward by $^{16}\text{O} \rightarrow ^{18}\text{O}$ substitution, as shown in Fig. 2. The energy dependence of $\Sigma_p(\mathbf{k}, \omega)$ is definitely due to the EPI introduced with the use of Eqs. (7), (11), and (12). Thus, we can conclude that in our solutions for all doping levels from the UD to the OD region, the dispersion kinks along the nodal direction are created *only when the EPI is included*.

Hereafter, we will discuss why the magnetic ingredients hardly bring the dispersion kinks along the nodal direction. Even when EPI does not exist, the electrons in our results are exposed to the strong AF fluctuation originating from the electronic correlation among d electrons. In Fig. 7, we show $\Sigma_d(\mathbf{k}, \omega)$ on the same six \mathbf{k} points as in Fig. 6. It is shown that there is no clear difference in $\Sigma_d(\mathbf{k}, \omega)$ between ^{16}O and ^{18}O materials. The energy dependence of $\Sigma_d(\mathbf{k}, \omega)$ is definitely due to the electronic correlation introduced with the use of Eqs. (8)–(10). We easily recognize that $\Sigma_d(\mathbf{k}, \omega)$ uniformly increases with the binding energy and has no maximal value up to 200 meV even for LD case, in which the strong AF fluctuation is expected to be grown. Thus, along the nodal direction, the strong AF fluctuation could cause the renormalization of the Fermi velocity, however, it hardly promotes any anomalous behavior such as kink structure.

Finally, we will discuss how our EEI affects the dispersion for ^{16}O materials. When the on-site Coulomb repulsion U is changed, the Fermi velocity is renormalized differently, but

this would not change the kink energy so much since the kink energy is determined by the EPI alone. In Fig. 8, we lay out our results for three different U s and they all correspond to OP. Their total doped holes δ are slightly different as: $\delta = 0.158, 0.154$, and 0.149 for $U = 2.5, 3.0$, and 3.5 eV, respectively. Hence, the Fermi momentum for $U = 2.5$ eV moves inside (or the Fermi surface shrinks) and the one for $U = 3.5$ eV moves outside (or the Fermi surface enlarges), compared to the one for $U = 3.0$ eV. These changes of the Fermi momenta are small; however, the dispersions at higher energy are quite affected, reflecting the binding energy dependence of $\Sigma_d(\mathbf{k}, \omega)$, as shown in Fig. 7. Therefore, the dispersion at higher energy could be changed a lot by the EEI even if the Fermi velocities are almost independent of them.

CONCLUSIONS

By the analysis of our model, we can show that the dispersion kink along the nodal direction occurs due to EPI. The isotope effect upon the electronic dispersion is shown near the kink of energy dispersion, not in the high binding energy portions.^{13,14} Our evaluation of the subtle isotope shifts has been backed by the report of the recent ARPES experiments^{16,17} which show the lack of the unusual isotope effect in the high energy portion.^{13,14,15} Fortunately for us, our scenario was possibly realized in further ARPES experiment.¹⁸ In addition to that, we have investigated how EEI effects on the nodal dispersion. It can hardly affect the kink and the nodal Fermi velocity; however, it can change the dispersion at higher energy. Hence, EPI and EEI play different roles on the nodal energy dispersion, respectively.

Of course, our treatment of EEI is just suited for *weak coupling regime*, and all of our parameter sets employed might be far from the ones for *strong coupling regime*. If we investigate *strong coupling regime* with the use of another approach, the low energy structure corresponding to the superexchange J could appear in the dispersion. However, our results presented here suggest that the structure should appear as a broad peak at higher energy due to the frequency dependence of the strong AF fluctuation, which will grow into J . As we all know, other works have already derive qualitatively similar conclusions on the basis of other models. Some groups adopt t - J models^{19,20,21,22} and other groups do one-band HH models.^{23,24,25} Furthermore, other groups have succeeded in explaining the ARPES results.^{26,27,28,29,30,31} However, in our 2D three-band HH model, both the electron-electron

interaction among the d electrons and the EPI on p electrons are considered according to high- T_c materials. We believe that it is important that quantitatively consistent results with the ARPES experiments can be reproduced from such a model. The advantage will be when our analysis extends to the superconducting state, in which the p electrons play important roles as well as d electrons.

ACKNOWLEDGMENTS

The authors are grateful to H. Iwasawa and T. Yanagisawa for their stimulating discussions. The computation in this work was performed on Intel Xeon servers at NeRI in AIST.

* email address: shigeami@h3.dion.ne.jp

- ¹ A. Kaminski, M. Randeria, J. C. Campuzano, M. R. Norman, H. Fretwell, J. Mesot, T. Sato, T. Takahashi, and K. Kadowaki, *Phys. Rev. Lett.* **86**, 1070 (2001).
- ² A. Lanzara, P. V. Bogdanov, X. J. Zhou, S. A. Kellar, D. L. Feng, E. D. Lu, T. Yoshida, H. Eisaki, A. Fujimori, K. Kishio, J.-I. Shimoyama, T. Noda, S. Uchida, Z. Hussain, and Z.-X. Shen, *Nature (London)* **412**, 510 (2001).
- ³ X. J. Zhou, T. Yoshida, A. Lanzara, P. V. Bogdanov, S. A. Kellar, K. M. Shen, W. L. Yang, E. Ronning, T. Sasagawa, T. Kakeshita, T. Noda, H. Eisaki, S. Uchida, C. T. Lin, F. Zhou, J. W. Xiong, W. X. Ti, Z. X. Zhao, A. Fujimori, Z. Hussain, and Z.-X. Shen, *Nature (London)* **423**, 398 (2003).
- ⁴ Z.-X. Shen, A. Lanzara, S. Ishihara, and N. Nagaosa, *Philos. Mag.* **82**, 1394 (2002).
- ⁵ K. Terashima, H. Matsui, D. Hashimoto, T. Sato, T. Takahashi, H. Ding, T. Yamamoto, and K. Kadowaki, *Nat. Phys.* **2**, 27 (2006).
- ⁶ V. B. Zabolotnyy, S. V. Borisenko, A. A. Kordyuk, J. Fink, J. Geck, A. Koitzsch, M. Knupfer, B. Büchner, H. Berger, A. Erb, C. T. Lin, B. Keimer, and R. Follath, *Phys. Rev. Lett.* **96**, 037003 (2006).
- ⁷ A. A. Kordyuk, S. V. Borisenko, V. B. Zabolotnyy, J. Geck, M. Knupfer, J. Fink, B. Büchner, C. T. Lin, B. Keimer, H. Berger, A. V. Pan, S. Komiya, and Y. Ando, *Phys. Rev. Lett.* **97**,

- 017002 (2006).
- ⁸ J. Lee, K. Fujita, K. McElroy, J. A. Slezak, M. Wang, Y. Aiura, H. Bando, M. Ishikado, T. Matsui, J.-X. Zhu, A. V. Balatsky, H. Eisaki, S. Uchida, and J. C. Davis, *Nature (London)* **442**, 546 (2006).
 - ⁹ R. J. McQueeney, J. L. Sarrao, P. G. Pagliuso, P. W. Stephens, and R. Osborn, *Phys. Rev. Lett.* **87**, 077001 (2001).
 - ¹⁰ N. E. Bickers and D. J. Scalapino, *Ann. Phys. (N.Y.)* **193**, 206 (1989).
 - ¹¹ D. L. Feng, N. P. Armitage, D. H. Lu, A. Damascelli, J. P. Hu, P. Bogdanov, A. Lanzara, F. Ronning, K. M. Shen, H. Eisaki, C. Kim, J.-i. Shimoyama, K. Kishio, and Z.-X. Shen, *Phys. Rev. Lett.* **86**, 5550 (2001).
 - ¹² Y.-D. Chuang, A. D. Gromko, A. Fedorov, Y. Aiura, K. Oka, Yoichi Ando, H. Eisaki, S. I. Uchida, and D. S. Dessau, *Phys. Rev. Lett.* **87**, 117002 (2001).
 - ¹³ G.-H. Gweon, T. Sasagawa, S. Y. Zhou, J. Graf, H. Takagi, D.-H. Lee, and A. Lanzara, *Nature (London)* **430**, 187 (2004).
 - ¹⁴ G.-H. Gweon, S. Y. Zhou, M. C. Watson, T. Sasagawa, H. Takagi, and A. Lanzara, *Phys. Rev. Lett.* **97**, 227001 (2006).
 - ¹⁵ G.-H. Gweon, T. Sasagawa, H. Takagi, D.-H. Lee, and A. Lanzara, arXiv:0708.1027.
 - ¹⁶ J. F. Douglas, H. Iwasawa, Z. Sun, A. V. Fedorov, M. Ishikado, T. Saitoh, H. Eisaki, H. Bando, T. Iwase, A. Ino, M. Arita, K. Shimada, H. Namatame, M. Taniguchi, T. Masui, S. Tajima, K. Fujita, S. Uchida, Y. Aiura, and D. S. Dessau, *Nature (London)* **446**, E5 (2007).
 - ¹⁷ H. Iwasawa, Y. Aiura, T. Saitoh, H. Eisaki, H. Bando, A. Ino, M. Arita, K. Shimada, H. Namatame, M. Taniguchi, T. Masui, S. Tajima, M. Ishikado, K. Fujita, S. Uchida, J. F. Douglas, Z. Sun, and D. S. Dessau, *Physica C* **463-465**, 52 (2007).
 - ¹⁸ H. Iwasawa, J. F. Douglas, K. Sato, T. Masui, Y. Yoshida, Z. Sun, H. Eisaki, H. Bando, A. Ino, M. Arita, K. Shimada, H. Namatame, M. Taniguchi, S. Tajima, S. Uchida, T. Saitoh, D. S. Dessau, and Y. Aiura (unpublished).
 - ¹⁹ O. Rösch and O. Gunnarsson, *Phys. Rev. Lett.* **92**, 146403 (2004).
 - ²⁰ S. Ishihara and N. Nagaosa, *Phys. Rev. B* **69**, 144520 (2004).
 - ²¹ A. S. Mishchenko and N. Nagaosa, *Phys. Rev. Lett* **93**, 036402 (2004).
 - ²² A. S. Mishchenko and N. Nagaosa, *Phys. Rev. B* **73**, 092502 (2006).
 - ²³ S. Fratini and S. Ciuchi, *Phys. Rev. B* **72**, 235107 (2005).

- ²⁴ G. Sangiovanni, O. Gunnarsson, E. Koch, C. Castellani, and M. Capone, *Phys. Rev. Lett.* **97**, 046404 (2006).
- ²⁵ P. Paci, M. Capone, E. Cappelluti, S. Ciuchi, and C. Grimaldi, *Phys. Rev. B.* **74**, 205108 (2006).
- ²⁶ T. Cuk, F. Baumberger, D. H. Lu, N. Ingle, X. J. Zhou, H. Eisaki, N. Kaneko, Z. Hussain, T. P. Devereaux, N. Nagaosa, and Z.-X. Shen, *Phys. Rev. Lett.* **93**, 117003 (2004).
- ²⁷ T. P. Devereaux, T. Cuk, Z. X. Shen, and N. Nagaosa, *Phys. Rev. Lett.* **93**, 117004 (2004).
- ²⁸ G. Seibold and M. Grilli, *Phys. Rev. B* **72**, 104519 (2005).
- ²⁹ E. G. Maksimov, O. V. Dolgov, and M. L. Kubic, *Phys. Rev. B* **72**, 212505 (2005).
- ³⁰ W. Meevasana, N. J. C. Ingle, D. H. Lu, J. R. Shi, F. Baumberger, K. M. Shen, W. S. Lee, T. Cuk, H. Eisaki, T. P. Devereaux, N. Nagaosa, J. Zaanen, and Z.-X. Shen, *Phys. Rev. Lett.* **96**, 157003 (2006).
- ³¹ R. Heid, K.-P. Bohnen, R. Zeyher, and D. Manske, *Phys. Rev. Lett.* **100**, 137001 (2008).